5 K Extended X-ray Absorption Fine Structure and 40 K 10-s Resolved Extended X-ray Absorption Fine Structure Studies of Photolyzed Carboxymyoglobin†

Tsu-Yi Teng,‡ Huey W. Huang,* and Glenn A. Olah
Physics Department, Rice University, Houston, Texas 77251
Received June 4, 1987; Revised Manuscript Received July 30, 1987

ABSTRACT: A previous extended X-ray absorption fine structure (EXAFS) study of photolyzed carboxymyoglobin (MbCO) [Chance, B., Fischetti, R., & Powers, L. (1983) *Biochemistry 22*, 3820–3829; Powers, L., Sessler, J. L., Woolery, G. L., & Chance, B. (1984) *Biochemistry 23*, 5519–5523] has provoked much discussion on the heme structure of the photoproduct (Mb*CO). The EXAFS interpretation that the Fe–CO distance increases by no more than 0.05 Å following photodissociation has been regarded as inconsistent with optical, infrared, and magnetic susceptibility studies [Fiamingo, F. G., & Alben, J. O. (1985) *Biochemistry 24*, 7964–7970; Sassaroli, M., & Rousseau, D. L. (1986) *J. Biol. Chem. 261*, 16292–16294]. The present experiment was performed with well-characterized dry film samples in which MbCO molecules were embedded in a poly(vinyl alcohol) matrix [Teng, T. Y., & Huang, H. W. (1986) *Biochim. Biophys. Acta 874*, 13–18]. The sample had a high protein concentration (12 mM) to yield adequate EXAFS signals but was very thin (40 μm) so that complete photolysis could be easily achieved by a single flash from a xenon lamp. Although the electronic state of Mb*CO resembles that of deoxymyoglobin (deoxy-Mb), direct comparison of EXAFS spectra indicates that structurally Mb*CO is much closer to MbCO than to deoxy-Mb. Our EXAFS analysis shows that photolysis of MbCO at 5 K leads to a stable intermediate state in which CO has moved away from iron by a distance of 0.27–0.45 Å, but the 5-coordinate heme structure is strained in a form similar to that of MbCO; the resolution of the CO position depends on the structure parameters of MbCO which we use as a reference for the analysis of Mb*CO. At 40 K, from 1 to 10 s after photolysis, 42% of the photoproduct has relaxed to the ground state, and the EXAFS spectrum of the remaining photoproduct is indistinguishable from that of the 5 K photoproduct.

Although it has been known for some time that the cooperative ligand binding to hemoglobin is mediated by protein conformation changes—that is to say, ligand binding induces changes in the protein conformation and these changes in turn modulate the ligand binding energy—the dynamic pathway relating ligand binding to protein structure changes is yet to be clarified. It appears that the structural dynamics of a hemoprotein following a ligand binding or release is exceedingly complex [Ansari et al. (1987) and references cited therein]. Therefore, it is desirable to decompose the dynamic process into elementary steps, especially for the reaction around the heme. This has been the goal of many recent theoretical and experimental studies of photolyzed carboxymyoglobin. The methods of these studies included EXAFS[1] (Chance et al., 1983; Powers et al., 1984), resonance Raman (Sassaroli et al., 1986; Rousseau & Argade, 1986), optical absorption (Iizuka et al., 1974), Mössbauer (Spartalian et al., 1979), magnetic susceptibility (Roder et al., 1984), and infrared measurements (Alben et al., 1982; Fiamingo & Alben, 1985). Of all the spectroscopies used, only EXAFS is capable of providing direct structural information. However, it has been argued that the results of the previous EXAFS study (Chance et al., 1983; Powers et al., 1984) are in disagreement with other low-temperature studies of photolyzed carboxymyoglobin (Fiamingo & Alben, 1985; Sassaroli & Rousseau, 1986). The results of Chance and Powers' 4 K EXAFS measurement were as follows: in MbCO the average length of the iron–porphinato nitrogen ($Fe–N_p$) bonds was 2.01 Å, the length of the iron–imidazole nitrogen ($Fe–N_{im}$) bond was 2.20 Å, and the length of the bond between the iron and the carbon of CO [Fe–C(O)] was 1.93 Å; in the photolyzed MbCO (photoproduct or Mb*CO), the distances were 2.03 Å for $Fe–N_p$, 2.22 Å for $Fe–N_{im}$, and 1.97 Å for Fe–C(O). On the other hand, it was found that the optical spectrum of the photoproduct was only slightly different from that of deoxy-Mb (Iizuka et al., 1974; Ansari et al., 1985); the major vibrational frequency of CO was shifted, upon photodissociation of MbCO, by 88–94% of the difference between that of MbCO and that of free CO gas (Alben et al., 1985); and the iron in the photoproduct was in the high-spin state similar to that in deoxy-Mb (Roder et al., 1984). Since photolysis clearly breaks the chemical bond between the iron and the CO, it is hard to imagine that the CO could remain within 0.05 Å of the Fe–C(O) bond distance as found by EXAFS. Fiamingo and Alben (1985) proposed that either a significant fraction of MbCO molecules in the EXAFS sample failed to be photolyzed or the EXAFS data had insufficient sensitivity to distinguish between 5- and 6-coordinate hemes. Sassaroli and Rousseau (1986) used a computer simulation to suggest that the CO, upon photodissociation, moves to a position about 4 Å away from the iron atom.

In view of the uncertainties over the structure of the low-temperature photoproduct and the questions raised over the results of Chance et al. (1983) and Powers et al. (1984), we

† This work was supported in part by NIH Grant HL-32593, ONR Contract N00014-86-K-0087, and the Robert A. Welch Foundation. Research carried out at the National Synchrotron Light Source, Brookhaven National Laboratory, was supported (in part) by the U.S. Department of Energy, Divisions of Materials Sciences and Chemical Sciences (DOE Contract DE-AC02-76CH00016).

* Author to whom correspondence should be addressed.
‡ Present address: Department of Biochemistry, Cornell University, Ithaca, NY 14853.

[1] Abbreviations: EXAFS, extended X-ray absorption fine structure(s); MbCO, ferrous carboxymyoglobin; deoxy-Mb, ferrous myoglobin; Mb*CO, photolyzed carboxymyoglobin or simply photoproduct; Hb, hemoglobin; Hepes, 4-(2-hydroxyethyl)-1-piperazineethanesulfonic acid; PVA, poly(vinyl alcohol); ClFeTPP, α,β,γ,δ-tetraphenylporphine iron chloride.

0006-2960/87/0426-8066$01.50/0

recently measured the EXAFS of the photoproduct at 5 K with a well-characterized MbCO sample. We found that at 5 K the heme structure remains essentially unchanged upon photodissociation except for an increase of 0.27–0.45 Å in the Fe–C(O) distance; the resolution of the CO position depends on the structural parameters of MbCO, which we used as a reference for the Mb*CO analysis. More precisely, if MbCO has Fe–N_p = 1.96 Å, Fe–N_{im} = 2.12 Å, and Fe–C(O) = 1.90 Å, then the photoproduct has Fe–N_p = 1.96 Å, Fe–N_{im} = 2.19 Å, and Fe–C(O) = 2.35 Å; however, if MbCO has Fe–N_p = 2.00 Å, Fe–N_{im} = 2.20 Å, and Fe–C(O) = 1.90 Å, then the photoproduct has Fe–N_p = 1.98 Å, Fe–N_{im} = 2.18 Å, and Fe–C(O) = 2.17 Å. We also measured a 10-s resolved EXAFS of the photoproduct at 40 K. We found that, from 1 to 10 s after photolysis, 42% of the photoproduct had relaxed to the ground state, and the EXAFS spectrum of the remaining photoproduct was indistinguishable from that of the 5 K photoproduct.

One major difference between our experiment and the previous one by Chance et al. (1983) and Powers et al. (1984) is in the sample preparation. The sample for this type of experiment must meet the competing requirements of high transparency to light and of high concentration in protein so as to possess a sufficient Fe fluorescence yield. Standard myoglobin solutions are either too concentrated (not 100% photolyzable) or too dilute (water or glycerol absorbs too much X-ray) (Teng & Huang, 1986). Possible difficulties, i.e., failure to achieve 100% photolysis, in the optically thick solution samples used by Chance et al. (1984) were recently discussed by Fiamingo and Alben (1985). The logical solution to this problem is to prepare thin but highly concentrated samples so that each is photolyzable and a few of them together would yield a sufficient X-ray signal. In an X-ray absorption experiment, a number of such samples can be spaced out in the direction of the incident X-ray beam so that each thin sample can be independently illuminated; the X-ray absorption or the X-ray fluorescence yield is then adjusted by the total thickness of the samples. We succeeded in preparing such thin samples by embedding MbCO molecules in dry poly(vinyl alcohol) (PVA) films and proved that MbCO in PVA film has the same properties as in frozen buffer solution by using optical absorption, ligand recombination kinetics, and EXAFS (Teng & Huang, 1986).

A few years ago, anticipating the availability of synchrotron radiation beams with intensities $\geq 10^{12}$ photons/(s·eV), we built a time-resolved EXAFS spectrometer (Huang et al., 1983; Liu et al., 1983). The idea was simple: one measures, at a given X-ray energy, a time sequence of EXAFS points before and after sample excitation and repeats the process at as many different energies as necessary. In order to perform such measurements efficiently, it is essential to use the integration method rather than the counting method for the measurements of both I_0 (the incident intensity) and I (the fluorescence intensity). [The photon statistics of this problem was discussed in Huang (1984).] The necessity of measuring the time-resolved spectrum energy point by energy point is a drawback compared to an energy dispersive method. However, the latter is not applicable to fluorescence EXAFS. To date, this point by point method remains the only practical way of measuring time-resolved fluorescence EXAFS.

In practice, the scarcity of high-intensity synchrotron radiation beam time and the instability problems of the synchrotron radiation beams in general (mainly due to the lack of fine control on the electron orbit in the storage ring) make a time-resolved experiment exceedingly difficult. We noted from the CO recombination curves of photolyzed MbCO [e.g., Austin et al. (1975)] that at 40 K the condition of the photoproduct varied only slightly during the time interval from about 1 to 10 s after photolysis. We therefore performed a time-resolved EXAFS measurement by integrating the EXAFS signals from ~1 to 10 s following photolysis (for simplicity, we call it a 10-s resolved measurement). In order to ensure that the sample had completely relaxed to the ground state before each flash photolysis, the temperature was raised to 120 K after the measurement of each energy point. In the following, we describe in detail the experiments and the data analysis.

Experimental Procedures

Samples. The method of preparing dry film samples with MbCO embedded in a PVA polymer matrix was described in a previous paper (Teng & Huang, 1986). It was shown there that such film samples have many desirable qualities: (1) MbCO embedded in the PVA matrix has the same properties as in a frozen buffer solution as mentioned above, (2) they are stable, easy to handle (for example, they may be exposed to air in room temperature for days without detectable change in properties), and resistant to radiation damage, (3) protein concentration can be as high as 15 mM, (4) light transparency is as good as liquid solution, but unlike a solution sample which often cracks at low temperatures, the light transmission property of a film does not change with temperature, and (5) the film can be made as thin as 20 μm so that 100% photolysis across a film, even with a high protein concentration, is easily achieved. The samples used in this experiment were made from crystalline myoglobin (type 2, sperm whale Mb, iron content approximately 0.29%) purchased from Sigma (St. Louis, MO) with Hepes as the buffer. Poly(vinyl alcohol), $[-CH_2CH(OH)-]_n$, had an average molecular weight around 40 000. Film samples of MbCO were prepared according to the aforementioned procedure to have a thickness about 40 μm and a protein concentration of 12 mM. MbCO solution samples used the same solution as used in making the films except PVA was omitted. Deoxy-Mb solution samples were prepared similarly to MbCO solutions except CO was not introduced in the process. Film samples of ClFeTPP were prepared by mixing 500 mg of ClFeTPP powder and 3.0 g of PVA into 14 mL of Hepes buffer (0.1 M, pH 7.6); the mixture was boiled and then dried at room temperature to a 100–150 μm thick film (final TPP concentration about 47 mM).

Flash and Temperature Control. Although we had shown that our film samples of MbCO had the desirable quality of being 100% photolyzable (Teng & Huang, 1986), it was quite another matter to maintain the sample control in a cryostat. In other words, we had to prove that under the condition of the X-ray experiment the sample was indeed photolyzed and the temperature of the sample was not changed significantly by the flash. This was handled by a specially designed cryostat. A small vacuum chamber with an interior radiation shield was connected to a liquid helium transfer line (which extended into a cold finger) and provided three X-ray windows (for incidence, transmission, and fluorescence), one flash window, and two optical windows for a light absorption monitor. The geometry of this arrangement is shown in Figure 1. The major components of this sample chamber included the following:

(1) SuperTran liquid helium transfer line was purchased from Janis Research Co. (Wilmington, MA), with a temperature range from 4 to 300 K at the cold finger. (Refrigeration capacity was >2 W at 4 K, cool-down time ~15 min from 300 to 4 K, and liquid consumption ~0.7 L/h at 4 K.) The temperature was controlled by a DRC-81C controller with

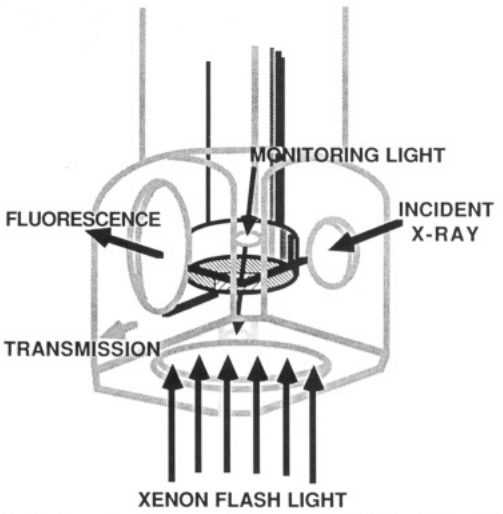

FIGURE 1: Schematic diagram of the sample holder. For clarity, the sample mount is not shown (see Figure 2).

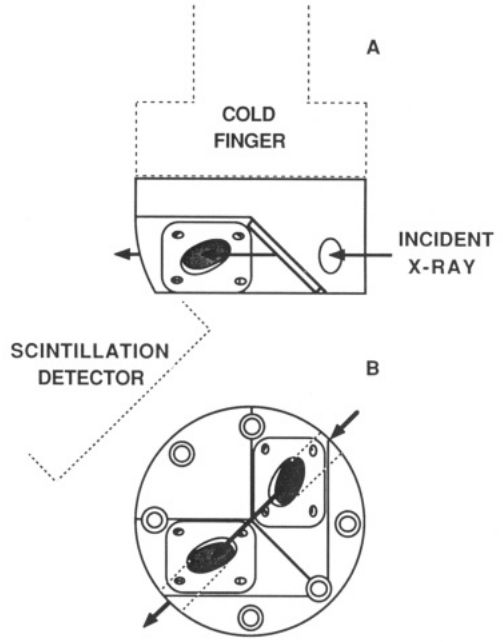

FIGURE 2: Schematic diagram of the sample mount: (A) side view; (B) bottom view.

a DT-500DRC-D silicon diode sensor (Lake Shore Cryotronics, Inc., Westerville, OH).

(2) A sample mount was made of cooper with a wedge-shaped cutout facing the scintillation detector (Figure 2). A circular hole was made through the mount for the passage of the X-ray beam such that on each of the two side faces of the wedge-shaped cutout there was an elliptical hole ($\sim$5 mm $\times$ 7 mm). A thin copper plate with a matching elliptical hole served as a frame. A film sample was sandwiched between a side face and a frame; four screws fastened the frame to the mount to ensure a good thermal contact between them. Also, a small amount of vacuum grease was applied to the surface of the film where it contacted copper to facilitate thermal conduction. The sample mount was fastened to the cold finger by six screws. Both films were oriented 45° vertically away from the incident beam first and then rotated 45° about a horizontal axis through the film so that the X-ray thickness was $\sqrt{3}$ times the film thickness. A second silicon diode sensor monitored the temperature of the sample mount near the sample; the reading was the same as that of the cold finger thermometer. It was difficult to measure the exact temperature of the exposed portion of the film sample. In a preliminary experiment, we used a solution sample with a thermocouple sensor buried in the solution. In this case the sample temperature was 4 deg higher than the cold finger at the low temperature end and the difference decreased to less than 1 deg for temperatures above 50 K. However, the film sample had a much better thermal contact with the cold finger than the solution sample did. For this reason, we assume that the lowest film temperature was about 5 K (definitely below 8 K). More important than the precise value of the temperature was the fact that at this temperature the optical and X-ray absorption spectra of the photoproduct remained constant indefinitely. A similar sample mount was made for optical absorption measurement [with a hole in the mount made in the direction of the monitoring light (see Figure 1)]. We decided not to monitor the light absorption during the X-ray experiment since the monitoring light would excite the sample. However, the photolysis and the ligand recombination kinetics of the film samples were thoroughly tested in this sample chamber under the same conditions as the X-ray experiment.

(3) A xenon flash tube (FXQ-260-3) capable of delivering 200 J with an 85-μs pulse width was purchased from EG & G Electro-Optics (Salem, MA). The power supply for the tube had the characteristics of $V \leq 2$ kV and $C = 126$ μF with a 12-kV flash trigger pulse (initiated by a TTL signal from the data acquisition system with a delay time less than 10 μs).

(4) The flash light was focused toward the sample by a "cold mirror" (no. 61.4200, Rolyn Optics Co., Covina, CA), which transmitted red and longer wavelength light but reflected light of wavelength shorter than 650 nm. The flash window further filtered this light to a narrow band between 450 and 650 nm. This was achieved by a short path filter ("hot mirror", no. 60.5200, Rolyn Optics Co.) on the vacuum shroud and a long path filter (yellow glass filter no. 5149, Oriel Corp., Stratford, CT) on the radiation shroud. This combination of two filters allowed 80% of 550-nm light to pass through. This optical arrangement was designed to utilize the absorption peaks of MbCO around 550 nm for efficient photolysis but block out the other wavelengths to avoid unnecessary heating of the sample. The effect of a single flash on the sample temperature was tested. It was found that the temperature would rise a few degrees for $T < 20$ K but less than 1 deg for $T > 100$ K and the change would last for a few seconds after a flash of 200 J (pulse width 85 μs). If the flash was repeated less than one flash per second, the temperature change would not exceed 10 deg.

(5) The monitoring light for detecting the degree of recombination occurring in the photolyzed sample was introduced through a small optical window with a fiber optical illuminator. The incident light passing through a filter (350–500 nm) was directed perpendicularly to a film sample. The transmitted light guided by another fiber optical cable was filtered by a narrow band interference filter (439.5 $\pm$ 0.5 nm) and delivered to a photomultiplier. The photodetector was recorded with a waveform digitizer for time-resolved recording. When the energy output of the flash was set greater than 80 J, the flash-induced change in the absorption coefficient (at 439.5 nm) of a MbCO film sample reached a maximum value (essentially the same value as the spectral difference between MbCO and deoxy-Mb). Also, with the flash output set at 100 J, we saw the same flash-induced change in the absorption coefficient with or without a neutral density filter (20% reduction) covering the flash unit. This showed that the film sample in the chamber was completely photolyzed by a flash of more than 80 J. Throughout this

experiment, the energy output of the flash unit was set at 100 J per flash.

Synchrotron Radiation Experimental Setup. The experiments were performed at Beamline X23B in the National Synchrotron Light Source (NSLS, Brookhaven National Laboratories, Upton, NY). The line was equipped with a collimating mirror, a double-crystal monochromator (Si 111), and a focusing mirror (Kirkland et al., 1983, 1986). The vertical position of the second crystal was adjusted with the crystal angle so that the focal point of the beam (~1 mm × 2 mm) was stationary during an EXAFS scan. This feature made it convenient for setting up the sample chamber particularly if the chamber was, as in our case, connected to a liquid helium vessel. The X-ray detectors were ion chambers for the incident and transmitted beams and a single 1.5-in. (diameter) NaI scintillation detector positioned 2 in. from the sample at 90° horizontal with respect to the incident beam. The detectors were each connected to a current integrator as described in Huang et al. (1983) and Liu et al. (1983). The transmitted beam was used to record the EXAFS of an iron foil for the purpose of energy calibration. The iron foil was taped to the front of the transmission ion chamber, so that the iron EXAFS was recorded simultaneously with the fluorescence EXAFS of the sample. The iron foil was positioned as far away as possible from the sample chamber to prevent the fluorescence of the foil from entering the chamber. During the EXAFS experiments, particularly when the sample temperature was below 120 K, the experimental hutch was kept dark in order to prevent stray light from exciting the sample.

5 K EXAFS. Fe K-edge EXAFS of MbCO film samples were measured before and after one flash or several flashes. The observed near-edge spectral changes due to photodissociation were independent of the number of flashes. At 5 K the spectrum of the photoproduct remained the same in time. To bring the photoproduct back to its ground state, i.e., MbCO, the sample was warmed to 120 K. A complete EXAFS spectrum from 100 eV below the Fe K edge to 650 eV above the edge was scanned in the following fashion: −100 to −10 eV, 10 eV/step and 1 s/point; −10 to 50 eV, 1 eV/step and 2 s/point; 50–250 eV, 2 eV/step and 4 s/point; 250–650 eV, 4 eV/step and 4 s/point. The intensity of the monochromatized beam during the experiment was (1–5) × 10^{10} photons/s. Figure 3 shows the quality (signal to noise ratio) of the data.

40 K 10-s Resolved EXAFS. For each energy point, the EXAFS signal was integrated for 10 s before flash. After a flash ($t = 0$) the signal was integrated from $t \lesssim 1$ s to $t = 10$ s. This process was controlled by a microcomputer as described in Huang et al. (1983) and Liu et al. (1983). The sample was then warmed to 120 K to ensure the complete relaxation and cooled down to 40 K again. In the meantime the monochromator was moved to the next energy point, ready to repeat the above process. The temperature cycle took 12 min. The complete scan from 100 eV below the K edge to 650 eV above the edge took 24 beam h. The problem of radiation damage to myoglobin samples had been studied previously (Teng & Huang, 1986). During our experiment the beam was down several times a day, so our samples were changed frequently. No samples showed detectable damage by visual inspection or by optical absorption measurement.

EXAFS Analysis. The method we used for EXAFS analysis was described in detail in Lee et al. (1981) and Eisenberger et al. (1978). The procedure included (1) removing the background, (2) multiplying by k^3 (where k is the wavenumber of the photoelectron), (3) Fourier transform filtering,

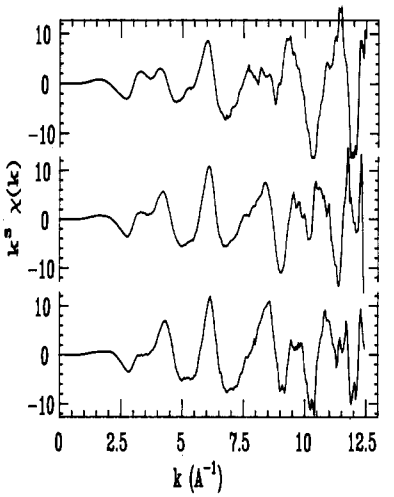

FIGURE 3: EXAFS spectra $k^3\chi(k)$ of MbCO (lower curve), Mb*CO (middle curve), and deoxy-Mb (upper curve). The data reduction procedure (background removal and conversion to k space) was applied to the X-ray absorption spectra (raw data).

(4) separating the amplitude and phase, and (5) decomposing a mixed shell. We used two independently written computer programs for steps 1–4 to test the dependence of the results on program. One was a part of our complete analysis program. The other, originating from University of Washington (UW EXAFS program library) and revised by Grant B. Bunker, was generously given to us by him. To test the consistency of our program, we first constructed artificial data of a heme based on theoretical phases and amplitudes (Lee & Beni, 1977; Lee et al., 1977; Teo & Lee, 1979) and then used our program to analyze them. The results were accurate within 0.005 Å. Data of MbCO obtained from different beamlines (X23B and X21A of NSLS and Beamline VII-3 of the Stanford Synchrotron Radiation Laboratory) were analyzed. The results agreed with each other within 0.007 Å. The results of using the UW program always agreed with our program within 0.01 Å for the first shell atomic distances and within 0.03 Å for the second shell atomic distances. The error estimates given below represent these values. We will only discuss the analysis of the first shell structures.

The method of Eisenberger et al. (1978) used for the decomposition of a mixed shell is as follows. Let R_1 be the Fe–N_p distance, Φ_1 the Fe–N_p phase shift + $2kR_1$, R_2 the Fe–N_{im} distance, φ^N the Fe–N phase shift, R_3 the Fe–C(O) distance, and φ^C the Fe–C phase shift. Also, let the phase of $k^3\chi(k)$ be denoted as $\Phi_1 + \Psi$, where $\chi(k)$ is the Fourier-filtered first shell EXAFS. Assume that the inelastic losses for a photoelectron backscattered from C and N atoms are approximately the same, that the Debye–Waller factors for all first shell atoms are the same, and that the backscattering amplitude is proportional to the atomic number of the target atom for $k \geq 4$ Å^{-1}. It can then be shown that

$$\Psi = \tan^{-1}\left\{\left[\frac{R_1^2}{4R_2^2}\sin\left[2k(R_2 - R_1)\right] + \frac{6R_1^2}{28R_3^2}\sin\left[2k(R_3 - R_1) + \varphi^C - \varphi^N\right]\right] \Big/ \left[1 + \frac{R_1^2}{4R_2^2}\cos\left[2k(R_2 - R_1)\right] + \frac{6R_1^2}{28R_3^2}\cos\left[2k(R_3 - R_1) + \varphi^C - \varphi^N\right]\right]\right\} \quad (1)$$

A similar equation can be written for a 5-coordinate heme. A key parameter in this analysis is the threshold energy E_0,

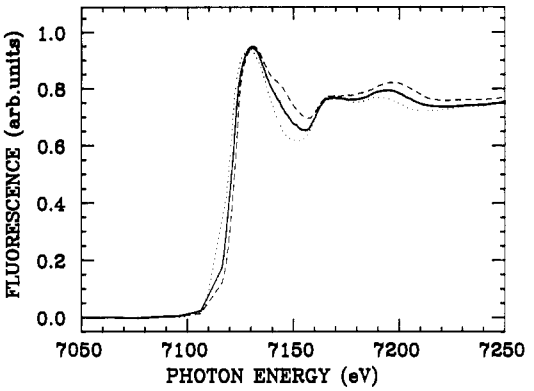

FIGURE 4: Near-edge spectra of MbCO (dashed line), Mb*CO (solid line), and deoxy-Mb (dotted line).

through which k was calculated from the X-ray energy. If R_2 and R_3 are known, either from single-crystal diffraction studies or from assumptions, one may input a value for R_1 to calculate Ψ. The *solution* for R_1 is obtained if the following two criteria are satisfied. Criterion 1: The linear fit to the quantity [phase of $k^3\chi(k)$] $- \Psi - \varphi^N$ as a function of k passes through the origin (Lee et al., 1981). Criterion 2: If criterion 1 is satisfied, R_1 calculated from the slope of the linear fit is the same as the input value.

We searched for the solution by varying E_0 over a reasonable range (Lee et al., 1981). Since the majority of the first shell atoms are nitrogen, the phase shift function φ^N is important. We extracted this function from the EXAFS of ClFeTPP. This was done by using the known Fe–N_p and Fe–Cl distances from X-ray diffractions (Hoard et al., 1967) and the theoretical Fe–Cl phase shift (Teo & Lee, 1979). The phase shift φ^C was also obtained from Teo and Lee (1979). This method of decomposition was first applied to hemoglobin by Eisenberger et al. (1978); the results agreed with a subsequent study using a method of curve fitting by Perutz et al. (1982).

RESULTS

Results Independent of EXAFS Analysis. Figure 4 shows the near-edge spectra of MbCO, Mb*CO at 5 K, and deoxy-Mb at 300 K. Two features are evident—namely, the edge shifts and the spectral differences from the peaks (~7130 eV) to 7200 eV. They were first observed and discussed by Chance et al. (1983). The spectrum of MbCO changed to that of Mb*CO after one flash (total output 100 J). Repeating flashes or increasing the flash energy did not change the spectrum further. However, if the flash energy was reduced below 80 J, a spectrum between MbCO and Mb*CO was obtained. In this case, repeating flashes eventually changed the spectrum toward that of Mb*CO. This and the optical absorption experiment mentioned earlier showed that complete photolysis of the sample was achieved by one flash (of 100 J).

A distinct presence of a bump at 7145 eV in the MbCO spectrum and its absence in both the Mb*CO and deoxy-Mb spectra make it clear that Mb*CO is not a mixture of MbCO and deoxy-Mb. In other words, Mb*CO is a well-defined intermediate state with its own characteristic X-ray absorption spectrum different from that of MbCO or deoxy-Mb. The shifts of the edge energy are consistent with the elementary notion of quantum mechanics; since the coordination shell of deoxy-Mb is more open than that of MbCO, the energy levels of the outer orbitals of the iron are lower in deoxy-Mb than in MbCO (Dutta & Huang, 1980). The heme structure of Mb*CO is obviously somewhere in between. Deoxy-Mb is red-shifted from MbCO by 2–2.5 eV, whereas Mb*CO is red-shifted by about 1 eV.

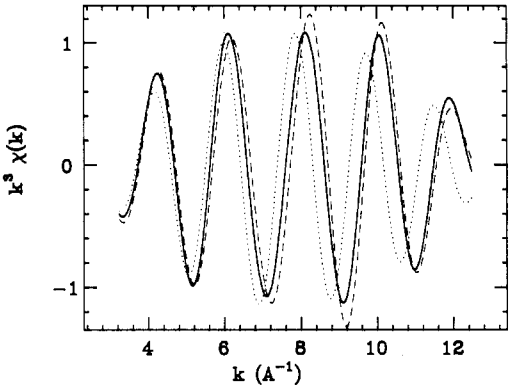

FIGURE 5: First shell EXAFS $k^3\chi(k)$ of MbCO (dashed line), Mb*CO (solid line), and deoxy-Mb (dotted line) obtained from Figure 3 by Fourier transform filtering. All three spectra were obtained by the same reduction procedure with the same E_0.

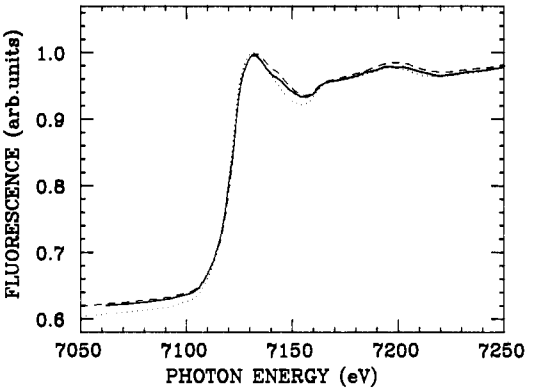

FIGURE 6: Near-edge absorption spectra of MbCO (dashed line; at 40 K), 40 K photoproduct 1–10 s after flash (solid line), and 5 K photoproduct (dotted line).

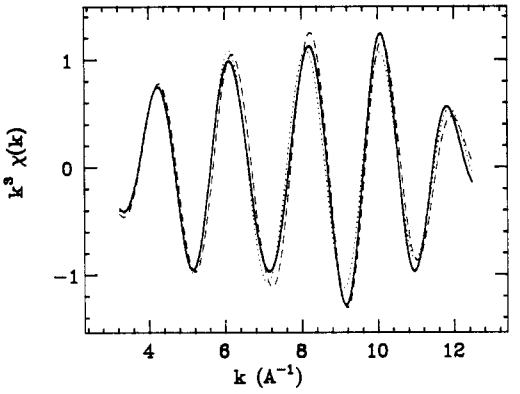

FIGURE 7: First shell EXAFS $k^3\chi(k)$ of MbCO (dashed line; at 40 K), 40 K photoproduct 1–10 s after flash (solid line), and 5 K photoproduct (dotted line). All three spectra were obtained by the same reduction procedure from the raw data with the same E_0.

Figure 5 shows the first shell EXAFS obtained from Figure 3 by Fourier transform filtering. It is clear from the comparison of these three spectra that the structure of Mb*CO is much closer to that of MbCO than to that of deoxy-Mb.

The 10-s resolved EXAFS at 40 K taken before and after the flash are shown in Figures 6 and 7 along with the EXAFS of the 5 K photoproduct. Figure 6 shows the near-edge spectra and Figure 7 the Fourier-filtered first shell EXAFS. A one-parameter linear combination of MbCO and 5 K Mb*CO was made to fit the 40 K photoproduct. The best fit was given by 42% MbCO and 58% 5 K Mb*CO. This is in agreement with the transient optical absorption studies (Austin et al., 1975), which show that 60% of the photodissociated MbCO at 40 K remains unbound from 1 to 10 s after photolysis. We subtracted 42% MbCO from the 40 K photolyzed spectrum and

Table I: Heme Structure by Single-Crystal X-ray Analysis (X) and by EXAFS (E)

complex	R_1, Fe–N_p (Å)	R_2, Fe–N_{im} (Å)	R_3, Fe–ligand (Å)	2nd shell Fe–C (Å)	2nd shell $(\sigma^2 - \sigma^2_{TPP})^a$ (10^{-3} Å^2)	method, ref
MbCO	1.97	2.2	1.9			X, Kuriyan et al. (1986)
MbO_2	1.95 ± 0.06	2.07 ± 0.06	1.83 ± 0.06			X, Philips (1980)
deoxy-Mb	2.06	2.1				X, Takano (1977)
deoxy-Hb	2.06 ± 0.02	2.12 ● 0.04				X, Fermi et al. (1984)
MbCO	2.00 ± 0.01	[2.20]^b	[1.90]	2.98 ± 0.03	−2.7	E, 5 K film^c
Mb*CO	1.98 ± 0.01	2.18 ± 0.01	2.17 ± 0.01			
MbCO	1.96 ± 0.01	[2.12]	[1.90]			E, 5 K film^c
Mb*CO	1.96 ± 0.01	2.19 ± 0.01	2.35 ± 0.01			
deoxy-Mb	2.06 ± 0.01	[2.1]			2.3	E, 300 K solution^c
MbCO	2.01 ± 0.02	2.20 ± 0.02	1.93 ± 0.02			E, Powers et al. (1984)
Mb*CO	2.03 ± 0.02	2.22 ± 0.02	1.97 ± 0.02			E, Powers et al. (1984)

^{a} σ^2 is a Debye–Waller factor for an interatomic distance and σ^2_{TPP} that of ClFeTPP in PVA film at 300 K. ^{b} The quantities in brackets are inputs in the EXAFS analysis. ^{c} Results from this work. A brace indicates a set of solutions.

found the remaining spectrum indistinguishable from 5 K Mb*CO within experimental error.

Results of EXAFS Analysis. To test the analysis program, we first analyzed deoxy-Mb and compared our result with the X-ray diffraction result (Takano, 1977). This was done by using the crystallographical distance R_2 = 2.1 Å. The method of decomposition of a mixed shell gave R_1 = 2.06 Å, in perfect agreement with the crystallographical result.

Since the EXAFS of MbCO and Mb*CO were obtained from the same sample and under the same experimental conditions, they are ideal for structural comparison. Table I includes the crystallographical results of four different ferrous hemes: MbCO, MbO_2, deoxy-Mb, and deoxy-Hb. However, the axial ligand distances R_2 (Fe–N_{im}) and R_3 [Fe–C(O)] of MbCO were known only to two digits. In comparison with the other ferrous hemes, R_2 = 2.2 Å for MbCO (Kuriyan et al., 1986) seems a little large. Accordingly, in the analysis of MbCO EXAFS, we used two sets of axial ligand distances, set A with R_2 = 2.20 Å and R_3 = 1.90 Å and set B with R_2 = 2.12 Å and R_3 = 1.90 Å, to cover a possible range of R_2. The method of decomposition gave the solution of R_1 = 2.00 Å for set A and R_1 = 1.96 Å for set B, which are in general agreement with the crystallographical distance R_1 = 1.97 Å. One might, at first sight, expect a smaller R_1 for a larger R_2. This was not so because the solution for set A was found at a value of E_0 that was 9 eV larger than E_0 for set B. The role of the threshold energy E_0 as an adjustable parameter in EXAFS analysis has been discussed at length in Lee et al. (1981). It is not unreasonable for E_0 of a complex system to have an adjustable range of 10 eV. On the other hand, because of the high accuracy of the spectral difference between MbCO and Mb*CO, it is reasonable to expect their E_0's to be consistent with the experimental edge shift, i.e., E_0(Mb*CO) ≅ E_0(MbCO) − 1 eV. (The relation between deoxy-Mb and MbCO is more complicated; MbCO involves an additional atom and an additional phase shift φ^C. Therefore, no relation between their E_0's was imposed).

5 K Mb*CO was first analyzed as a 5-coordinate heme, but no acceptable solution was found. We then searched for 6-coordinate solutions by varying R_2 in the range of 2.12–2.20 Å and R_3 in the range of 1.83–2.50 Å while E_0 was fixed at 1 eV below that of MbCO. The result of using the MbCO structure R_1 = 2.00 Å, R_2 = 2.20 Å, and R_3 = 1.90 Å as a reference is the following: R_1 = 1.98 Å, R_2 = 2.18 Å, and R_3 = 2.17 Å. The result of using the MbCO structure R_1 = 1.96 Å, R_2 = 2.12 Å, and R_3 = 1.90 Å as a reference is the following: R_1 = 1.96 Å, R_2 = 2.19 Å, and R_3 = 2.35 Å.

Discussion

It is well-known that, because of the various approximations as well as some degree of arbitrariness involved in data analysis, EXAFS is best used for structural comparison of similar compounds [see the details in Lee et al. (1981)]. Equally important is that the data for comparison should be taken, as closely as possible, under the same conditions (sample condition, beam condition, experimental setup, etc.). In these respects, we had in hand an ideal EXAFS study.

Although many spectroscopic studies have indicated that the electronic state of Mb*CO resembles that of deoxy-Mb, Figure 5 clearly shows that structurally Mb*CO is closer to MbCO than to deoxy-Mb. In making this comparison, we want to emphasize that the three spectra in Figure 5 were obtained from raw data by the same reduction program with the same E_0. And although the deoxy-Mb sample was a solution at 300 K while the other two were a film at 5 K, we had carefully compared the spectra of MbCO in solution at 300 K and in film at 300 and 5 K; we found that all three of them gave the same EXAFS (Teng & Huang, 1986).

Our analysis (summarized in Table I) indicates that photolysis moves the CO away from the iron atom for a distance in the range of 0.3–0.5 Å but leaves the 5-coordinate structure of heme essentially unchanged. We conclude that photolysis of MbCO at 5 K leads to a stable intermediate in which CO has dissociated and iron has changed to the high-spin state but the heme structure is strained in a form similar to MbCO. This intermediate state, as far as we could tell, remains the same at 40 K.

Thus our conclusion from the 5 K experiment differs substantially from that of Chance et al. (1983) and Powers et al. (1984); in their result, CO is displaced no more than 0.05 Å (radially) and therefore most likely remains within the Fe–C(O) bonding distance. However, we are not able to determine the source of the discrepancy between the present and the previous work (that is, whether it resides in the spectra themselves or only in the quantitative interpretation). Also, we noted that our data were not sensitive enough to determine the position of the oxygen atom of the CO.

Acknowledgments

We are grateful to John Olson for his advice and assistance in handling myoglobin and hemoglobin, John Kirkland and Rich Neiser for their expert assistance at Beamline X23B, NSLS, Grant Bunker for letting us use his EXAFS analysis program for comparison, and Jim Phillips for his assistance in conducting our preliminary experiments at Beamline X21A, NSLS.

Registry No. Fe, 7439-89-6; CO, 630-08-0; heme, 14875-96-8.

References

Alben, J. O., Beece, D., Bowne, S. F., Doster, W., Eisenstein, L., Frauenfelder, H., Good, D., McDonald, J. D., Marden,

M. C., Moh, P. P., Reinisch, L., Reynolds, A. H., Shyamsunder, E., & Yue, K. T. (1982) *Proc. Natl. Acad. Sci. U.S.A. 79*, 3744–3748.

Ansari, A., Berendzen, J., Bowne, S. F., Frauenfelder, H., Iben, I. E. T., Sauke, T. B., Shyamsunder, E., & Young, R. D. (1985) *Proc. Natl. Acad. Sci. U.S.A. 82*, 5000–5004.

Ansari, A., Berendzen, J., Braunstein, D., Cowen, B. R., Frauenfelder, H., Hong, M. K., Iben, I. E. T., Johnson, J. B., Ormos, P., Sauke, T. B., Scholl, R., Schulte, A., Steinbach, P. J., Vittitow, J., & Young, R. D. (1987) *Biophys. Chem. 26*, 337–355.

Austin, R. H., Beeson, K. W., Eisenstein, L., Frauenfelder, H., & Gunsalus, I. C. (1975) *Biochemistry 14*, 5355–5393.

Chance, B., Fischetti, R., & Powers, L. (1983) *Biochemistry 22*, 3820–3829.

Dutta, C. M., & Huang, H. W. (1980) *Phys. Rev. Lett. 44*, 643–646.

Eisenberger, P., Shulman, R. G., Kincaid, B. M., Brown, G. S., & Ogawa, S. (1978) *Nature (London) 274*, 30–34.

Fermi, G., Perutz, M. F., Shaanan, B., & Fourme, R. (1984) *J. Mol. Biol. 175*, 159–174.

Fiamingo, F. G., & Alben, J. O. (1985) *Biochemistry 24*, 7964–7970.

Good, N. E., Winget, G. D., Winter, W., Connolly, T. N., Izawa, S., & Singh, R. M. M. (1966) *Biochemistry 5*, 467–477.

Hoard, J. L., Cohen, G. H., & Glick, M. D. (1967) *J. Am. Chem. Soc. 89*, 1992–1996.

Huang, H. W. (1984) in *EXAFS and Near-Edge Structure* (Hodgson, K. O., Hedman, B., & Penner-Hahn, J. E., Ed.) Vol. III, pp 158–163, Springer-Verlag, Berlin.

Huang, H. W., Liu, W. H., Teng, T. Y., & Wang, X. F. (1983) *Rev. Sci. Instrum. 54*, 1488–1491.

Iizuka, T., Yamamoto, H., Kotani, M., & Yonetani, T. (1974) *Biochim. Biophys. Acta 371*, 126–139.

Kirkland, J. P., Nagel, D. J., & Cowan, P. L. (1983) *Nucl. Instrum. Methods Phys. Res. 208*, 49–54.

Kirkland, J. P., Neiser, R. A., & Elam, W. T. (1986) *Nucl. Instrum. Methods Phys. Res., Sect. A 246*, 203–206.

Kuriyan, J., Wilz, S., Karplus, M., & Petsko G. A. (1986) *J. Mol. Biol. 192*, 133–154.

Lee, P. A., & Beni, G. (1977) *Phys. Rev. B: Solid State 15*, 2862–2883.

Lee, P. A., Teo, B. K., & Simons, A. L. (1977) *J. Am. Chem. Soc. 99*, 3856–3859.

Lee, P. A., Citrin, P. H., Eisenberger, P., & Kincaid, B. M. (1981) *Rev. Mod. Phys. 53*, 769–805.

Liu, W. H., Wang, X. F., Teng, T. Y., & Huang, H. W. (1983) *Rev. Sci. Instrum. 54*, 1653–1656.

Perutz, M. F., Hasnain, S. S., Duke, P. J., Sessler, J. L., & Hahn, J. E. (1982) *Nature (London) 295*, 535–538.

Phillips, S. E. V. (1980) *J. Mol. Biol. 142*, 531–554.

Powers, L., Sessler, J. L., Woolery, G. L., & Chance, B. (1984) *Biochemistry 23*, 5519–5523.

Roder, H., Berendzen, J., Bowne, S. F., Frauenfelder, H., Sauke, T. B., Shyamsunder, E., & Weissman, M. B. (1984) *Proc. Natl. Acad. Sci. U.S.A. 81*, 2359–2363.

Rousseau, D. L., & Argade, P. V. (1986) *Proc. Natl. Acad. Sci. U.S.A. 83*, 1310–1314.

Sassaroli, M., & Rousseau, D. L. (1986) *J. Biol. Chem. 261*, 16292–16294.

Sassaroli, M., Dasgupto, S., & Rousseau, D. L. (1986) *J. Biol. Chem. 261*, 13704–13713.

Spartalian, K., Lang, G., & Yonetani, T. (1979) *Biochim. Biophys. Acta 428*, 281–290.

Takano, T. (1977) *J. Mol. Biol. 110*, 569–584.

Teng, T. Y., & Huang, H. W. (1986) *Biochim. Biophys. Acta 874*, 13–18.

Teo, B. K., & Lee, P. A. (1979) *J. Am. Chem. Soc. 101*, 2815–2832.